4-15-2006

Self-assembled nanocrystalline epitaxial manganite films on $SrTiO_3$/Si heterostructures

D. Hunter
Center for Materials Research, Norfolk State University, Norfolk, Virginia

J.B. Dadson
Center for Materials Research, Norfolk State University, Norfolk, Virginia

K. Zhang
Center for Materials Research, Norfolk State University, Norfolk, Virginia

B. Lasley
Center for Materials Research, Norfolk State University, Norfolk, Virginia

K. Lord
Center for Materials Research, Norfolk State University, Norfolk, Virginia

See next page for additional authors

Self-assembled nanocrystalline epitaxial manganite films on $SrTiO_3$/Si heterostructures

D. Hunter, J. B. Dadson, K. Zhang, B. Lasley, K. Lord, T. M. Williams, R. R. Rakhimov, and A. K. Pradhan[a)]
Center for Materials Research, Norfolk State University, 700 Park Avenue, Norfolk, Virginia 23504

J. Zhang and D. J. Sellmyer
Department of Physics and Astronomy and Center for Materials Research and Analysis, University of Nebraska, Lincoln, Nebraska 68588-0113

(Presented on 2 November 2005; published online 18 April 2006)

We report the growth and magnetic characterizations of $La_{0.7}Ba_{0.3}MnO_3$ and $La_{0.7}Sr_{0.3}MnO_3$ films on $SrTiO_3$-buffered Si (100) and Si (111) substrates by pulsed-laser deposition. The structural studies show the epitaxial nature of the films. The microscopic studies show that the films consist of nanocrystalline particles. All films display sharp magnetic and electrical transitions associated with the colossal magnetoresistance behavior at and above room temperature, illustrating the superior quality of the films. © *2006 American Institute of Physics*. [DOI: 10.1063/1.2162088]

Since the discovery of colossal magnetoresistance (CMR),[1,2] mixed valence manganites have received considerable research interest[1–6] due to their unique resistive and magnetic properties which facilitate potential applications in magnetic, magnetoelectronic, photonic devices as well as spintronic technology. The interplay among the spin, charge, and orbital degree of freedom in these materials[3–6] leads to many intriguing phenomena, such as metal-insulator transition, magnetic phase transition, and nanoscale electronic phase separation leading to percolative electron transport phenomena in the context of both charge and orbital ordering.[1–9] The perovskite lanthanum-based manganites ($R_{1-x}B_xMnO_3$, where R and B are rare-earth and alkaline metals, respectively) films have been grown on single-crystal oxide substrates, such as $SrTiO_3$ (STO), $LaAlO_3$ (LAO), and $NdGaO_3$. Although advances have been made in the preparation of nano- and microcrystalline manganites[10–16] on different substrates, films integrated onto Si and other potential semiconductors and their physical investigations have not been possible due to large substrate and film lattice mismatch, mechanical and chemical disaccords arising from the structural dissimilarities. Integration of manganites onto semiconducting materials such as on Si, remains a challenging task for potential device applications that utilize both information processing and data storage in the same device. The recent progresses on direct integration of STO on Si have opened the possibility to integrate both STO and $R_{1-x}B_xMnO_3$ onto this technologically important semiconductor. Here we report the growth of high-quality epitaxial $La_{0.7}Ba_{0.3}MnO_3$ (LBMO) and $La_{0.7}Sr_{0.3}MnO_3$ (LSMO) films grown on STO/Si (100/111) heterostructures using pulsed-laser deposition (PLD). The films demonstrate ferromagnetic properties in the vicinity of room temperature.

Epitaxial LBMO and LSMO nanocrystalline films were grown on STO-buffered Si substrates (both 100 and 111) by multitarget PLD technique (KrF excimer, $\lambda = 248$ nm) with a pulse energy density of 1–2 J/cm^2. Single-crystalline STO and high-density LBMO and LSMO targets were used. The manganite films were deposited with a substrate temperature of 700–800 °C, keeping oxygen partial pressure within 200–400 mTorr. However, for the growth of STO template layer on Si, the initial 2-nm-thick STO film was deposited without using oxygen gas. Subsequently, an 18-nm-thick film of STO was deposited with oxygen partial pressure of 1 mTorr with laser repetition rate of 3 Hz. Manganite films having thickness of 50–100 nm were immediately deposited on STO/Si using a laser repetition rate of 5 Hz. The films were cooled to room temperature in 1–2 Torr of oxygen partial pressure.

The films were characterized by x-ray diffraction (XRD) and atomic force microscopy (AFM). Magnetization (M) was measured by a superconducting quantum interference device (SQUID) magnetometer with in-plane magnetic field. Electrical transport was studied by a four-probe a.c. technique.

The overall crystalline structure was studied by XRD. In LBMO (or LSMO)/STO/Si heterostructures, LBMO grew epitaxially only in (200) direction as shown in Fig. 1. This is very consistent with the XRD pattern for LBMO or LSMO grown directly on STO substrate as shown in the inset of Fig. 1 for LBMO/STO film. The XRD patterns illustrate the highly crystalline and epitaxial nature of the films.

Figure 2 shows the AFM images of LBMO/STO/Si(100/111) and LSMO/STO/Si(100/111) which reveal that the surface is comprised of nanometer-sized particles. The typical size of the particles is about 20 nm, and the size distribution is very small, indicating the uniformity of all particles. The root-mean-square (rms) surface roughness is less than 2 nm in all films. Furthermore, the three-dimensional (3D) AFM images of the films reveal nanocone-like structures which are uniformly distributed over the surface. However, particle size for the LBMO/STO is about twice larger than the films grown on STO-buffered Si. The overall growth mode can be considered as Volmer-Weber

[a)]Electronic mail: apradhan@nsu.edu

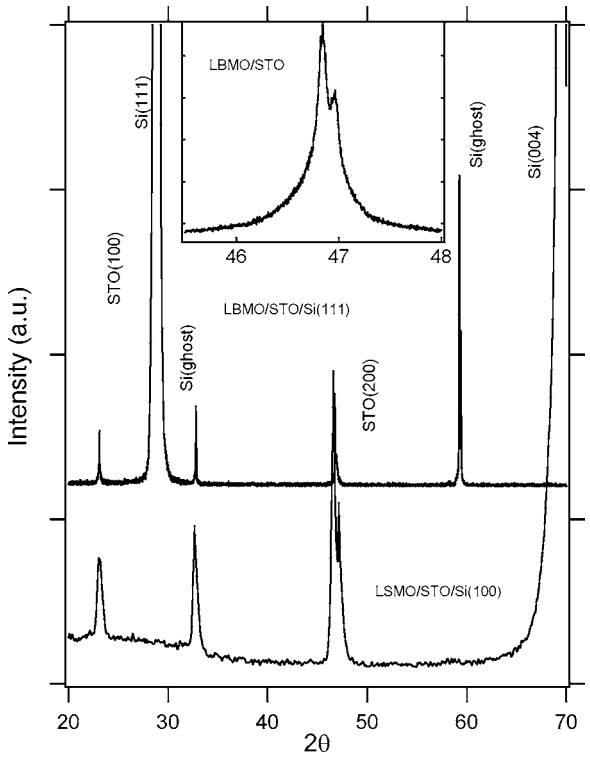

FIG. 1. X-ray diffraction (XRD) analysis of nanocrystalline LBMO (LSMO)/STO/Si films grown by pulsed-laser deposition. The inset shows the XRD pattern for LBMO/STO film.

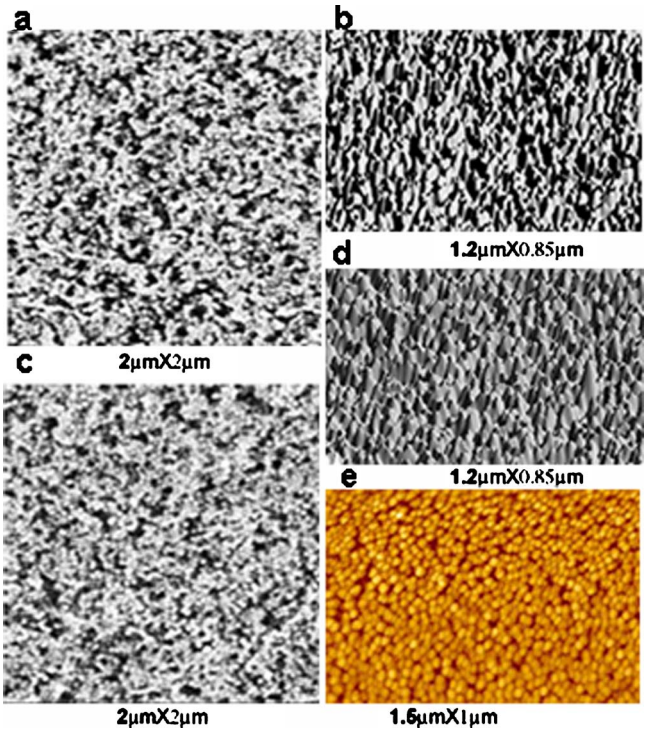

FIG. 2. Atomic force microscopic (AFM) observations of nanocrystalline films of manganites. (a) and (b) are the two-dimensional (2D) and 3D AFM images of LBMO/STO/Si(100), respectively. (c) and (d) are 2D and 3D AFM images of LBMO/STO/Si(111), respectively. The 2D images display very uniform nanocrystalline nature of the particle with particle size less than 20 nm. The 3D images reveal the self-assembled inverted nanocone structures uniformly distributed on the surface. (e) shows the nanocrystalline manganite film directly on STO substrate consisting of nanoparticles of about 40 nm in size.

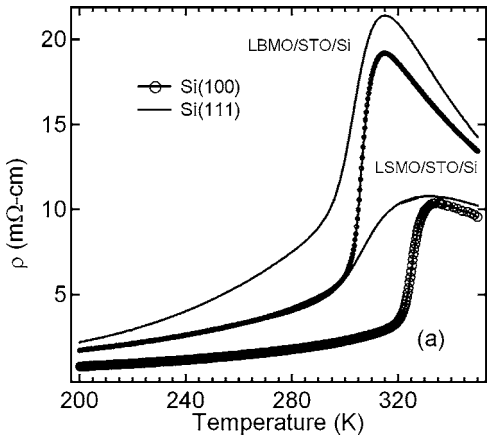

FIG. 3. The electrical resistivity of (a) LBMO and (b) LSMO films on Si(100) and Si(111) substrates.

growth in which the energy relaxation takes place via the formation of 3D islands to minimize the energy. If the strain energy is large, particularly compressive in nature as in manganites, the system will try to rearrange itself to find a lower-energy state favoring the formation of 3D islands which may consist of self-assembled nanocrystalline particles.

The corresponding zero-field resistivity results are also shown in Figs. 3(a) and 3(b) for both LBMO/STO/Si and LSMO/STO/Si multilayers, respectively. The temperature dependence of resistivity reveals a remarkable sharp jump at the metal-insulator transition temperature (T_{MI}) and is consistent with the magnetic transition.

The temperature dependence of the magnetization is shown in Fig. 4 for both LBMO and LSMO nanocrystalline films in a field of 0.1 T with the film surface parallel to the applied magnetic field. The magnetic transitions inferred from the zero-field-cooled (ZFC) magnetization for LBMO films grown both on Si(100) and Si(111) are fairly sharp with T_c=315 K as shown in Fig. 4. The ZFC magnetization for LSMO on both Si(100) and Si(111) shows the ferromagnetic transition of LSMO with T_c=330 K, which is fairly sharp. The magnetization results clearly show that the magnetic transitions in the above films are enhanced compared to those previously reported[17] on both LBMO/STO/MgO and LSMO/STO/MgO films. One of the reasons for such en-

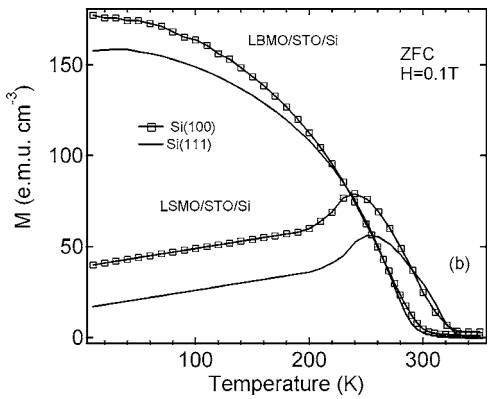

FIG. 4. The temperature dependence of the zero-field-cooled (ZFC) magnetization of LBMO/STO and LSMO/STO film on Si(100) and Si(111) substrates, indicating the transition temperature at 315 and 330 K, respectively.

hancement in T_c may be due to the strain relaxation in LBMO or LSMO films due to their nanocrystalline behavior.

In conclusion, $La_{0.7}Ba_{0.3}MnO_3$ and $La_{0.7}Sr_{0.3}MnO_3$ films were grown on $SrTiO_3$-buffered Si (100) and Si (111) substrates by pulsed-laser deposition. The films display epitaxial growth with self-assembled nanocrystalline particles. All films exhibit magnetic and electrical properties associated with the colossal magnetoresistance behavior at and above room temperature. These films may be useful for fabrication of potential devices.

ACKNOWLEDGMENTS

This work is supported by the NASA and NSF Center for Research Excellence in Science and Technology (CREST) Grant No. HRD-9805059. One of the authors (RRR) acknowledges support from the faculty research program provided by NASA. Research at the University of Nebraska is supported by NSF-MRSEC, ONR, and CMRA.

[1]S. Jin, T. H. Tiefel, M. McCormack, R. A. Fastnacht, and R. Ramesh, Science **264**, 413 (1994).
[2]R. von Helmholt, J. Wecker, B. Holszapfel, L. Schultz, and K. Samwer, Phys. Rev. Lett. **71**, 2331 (1993).
[3]A. Moreo, S. Yunoki, and E. Dagotto, Science **283**, 2034 (1999).
[4]M. Uehara, S. Mori, C. H. Chen, and S.-W. Cheong, Nature (London) **399**, 560 (1999).
[5]A. J. Millis, Nature (London) **392**, 147 (1998).
[6]Y. Tokura and N. Nagosa, Science **288**, 462 (2000).
[7]M. B. Salamon and M. Jaime, Rev. Mod. Phys. **73**, 583 (2001).
[8]M. Fath, S. Freisem, A. A. Menovsky, Y. Tomoika, J. Aarts, and J. A. Mydosh, Science **285**, 1540 (1999).
[9]J. C. London, N. D. Mathur, and P. A. Midgley, Nature (London) **420**, 797 (2002).
[10]P. Yang, T. Deng, D. Zhao, P. Feng, D. Pine, B. F. Chmelka, G. M. Whitesides, and G. D. Stucky, Science **282**, 2244 (1998).
[11]D. Zhu, H. Zhu, and Y. Zhang, Appl. Phys. Lett. **80**, 1634 (2002).
[12]J. J. Urban, L. Ouyang, M.-H. Jo, D. S. Wang, and H. Park, Nano Lett. **4**, 1547 (2004).
[13]J. Jiang, L. L. Henry, K. I. Gnansekar, C. Chen, and E. I. Meletis, Nano Lett. **4**, 741 (2004).
[14]V. Moshnyaga *et al.*, Nat. Mater. **2**, 247 (2004).
[15]S. Han *et al.*, Nano Lett. **4**, 1241 (2004).
[16]J.-H. Kim, S. I. Khartsev, and M. Grishin, Appl. Phys. Lett. **82**, 4295 (2003).
[17]A. K. Pradhan, D. Sahu, B. K. Roul, and Y. Feng, J. Appl. Phys. **96**, 1170 (2004).